

**One-step rapid synthesis of TS-1 zeolites with highly catalytic active mononuclear TiO₆ species**

Journal:	<i>Journal of Materials Chemistry A</i>
Manuscript ID	TA-ART-12-2019-013851.R1
Article Type:	Paper
Date Submitted by the Author:	14-Apr-2020
Complete List of Authors:	Xu, Wenjing; Jilin University, Zhang, Tianjun; Jilin University, Bai, Risheng; Jilin University, College of Chemistry Zhang, P; Dalhousie University , Chemistry Yu, Jihong; Jilin University, State Key Laboratory of Inorganic Synthesis and Preparative Chemistry

ARTICLE

One-step rapid synthesis of TS-1 zeolites with highly catalytic active mononuclear TiO₆ species

Wenjing Xu,^{‡a} Tianjun Zhang,^{‡ac} Risheng Bai,^a Peng Zhang,^c Jihong Yu^{*ab}

Received 00th January 20xx,
Accepted 00th January 20xx

DOI: 10.1039/x0xx00000x

Modulation and determination of the coordination environments of Ti active sites in titanasilicate zeolites are of key challenges in the rational design of high performance heterogeneous catalysts. Up to now, the highly catalytic active Ti species while not yet unambiguously determined is mainly constructed by the complex post-treated method which is hard to precisely control the distribution of created Ti species. Herein, we showcase a facile strategy for one step rapid synthesis of TS-1 (**MFI** framework type) zeolites with highly catalytic active Ti species via active seed-assisted microwave irradiation. The coordination environment and local structure of Ti species in TS-1 zeolites are investigated by UV-vis, UV-Raman and X-ray absorption spectroscopy. Significantly, according to the elaborate characterizations based on extended X-ray absorption fine structure (EXAFS), such highly catalytic active Ti species has been clearly identified as novel mononuclear TiO₆ species. Experimental studies reveal that the active seeds can provide plenty of high-coordinated Ti precursors which play a critical role in creating mononuclear TiO₆ in zeolite framework coupled with microwave irradiation. Moreover, such mononuclear TiO₆ species remain stable upon calcination. The obtained catalyst affords a high turnover number value (272) in 1-hexene epoxidation reaction which is almost 70% higher than that of conventional TS-1 zeolite (161). This work may open new perspectives for the designed synthesis and applications of titanasilicate zeolite catalysts in various important selective oxidation reactions.

Introduction

Zeolites are a unique class of crystalline porous materials with well-defined pores and channels at molecular level, which are found a variety of applications in the chemical industry.¹⁻³ As one of the most important members of zeolite family, Ti-containing zeolites have been studied extensively with regards to a series of selective oxidation reactions, such as alkene epoxidation,⁴⁻⁸ ketone ammoximation,⁹ phenol oxidation,¹⁰ etc.

To enhance the catalytic performance of such catalysts, great efforts have been made in tailoring the crystal sizes or building hierarchical structures of Ti-containing zeolites, such as TS-1 (**MFI**), Ti-**MWW**, Ti-**MOR** and Ti-Beta (***BEA**).¹¹⁻¹⁶ However, as a key factor in the catalytic reactions, the exact nature of different Ti active sites remains unclearly unraveled. Density functional theory (DFT) calculations showed that a new kind of Ti sites which are located at adjacent Si vacancies in the TS-1

lattice were more reactive than fully coordinated Ti sites in propylene epoxidation.¹⁷ This finding pointed out a promising way to improve the catalytic performance of Ti-containing zeolites, namely, tuning the chemical environment of Ti active centers. Typically, an increase in the Lewis acid strength of titanium species and the adjustment of the Ti coordination states can both lead to tellingly enhancement in catalytic behaviors.¹⁸⁻²²

To date, several strategies have been proposed to modify the Ti active centers in Ti-containing zeolites.²³⁻²⁷ For instance, Fang and co-workers reported a strategy to increase the electropositivity of Ti active sites in Ti-**MWW** zeolite by implanting F species on the neighboring framework Si, and thus the catalytic property of such Ti species was enhanced.²³ However, the simultaneously formed harmful F species which lowered the catalytic property of Ti active sites must be eliminated afterwards. To overcome the complex synthetic procedure, in some other cases, the Ti active sites were directly modified via post-treatment approach. For instance, pentahedrally and octahedrally coordinated Ti species can be obtained by hydrothermal treatment of conventional tetra-coordinated Ti-containing zeolites with different organic amines.²⁴⁻²⁶ Meanwhile, with the development of modern characterization techniques, the local structures of different Ti active sites have been thoroughly investigated.²⁸⁻³² Notably, the unique mononuclear TiO₆ in TS-1 established based on UV-Raman and DFT calculations was proposed to be responsible for its excellent catalytic activity in alkenes epoxidation.^{18, 25-26}

^a State Key Laboratory of Inorganic Synthesis and Preparative Chemistry, College of Chemistry, Jilin University, Changchun 130012, P. R. China. E-mail: jihong@jlu.edu.cn

^b International Center of Future Science, Jilin University, Changchun 130012, P. R. China

^c Department of Chemistry, Dalhousie University, Halifax, Nova Scotia B3H 4R2, Canada.

Electronic supplementary information (ESI) available: More details of experimental and characterization processes, SEM images, textural properties, UV-vis spectra, UV-Raman spectra, XPS spectra, FT-IR spectra and the EXAFS fitting results of different TS-1 zeolites and the results of 1-hexene epoxidation reactions over TS-1-CM and TS-1-AM are provided.

[‡] These authors contributed equally.

Therefore, facile construction as well as elaborate identification of mononuclear TiO_6 has attracted considerable attention in exploring high-performance Ti-containing zeolite catalysts.

Compared with conventional hydrothermal synthesis of zeolites, microwave synthesis method has proven to be a more efficient way to prepare titanosilicate zeolites since the heat-up time can be rapidly and uniformly induced by the microwave irradiation.³³ On the other hand, seed-assisted method has demonstrated its significant impact on the distribution of Ti species. For instance, the surface Ti-enriched TS-1 zeolite can be obtained via seed-assisted intermediate crystallization strategy.³⁴ In this work, we developed a one-step method to rapidly synthesize TS-1 zeolites with highly catalytic active mononuclear TiO_6 species. By introducing active seeds which can provide plenty of highly coordinated Ti precursors with the assistance of microwave irradiation, highly crystalline TS-1 zeolites containing mononuclear TiO_6 can be prepared within 1 hour. Significantly, based on X-ray absorption spectroscopy (XAS), we clearly identified the mononuclear state of TiO_6 species in the TS-1 zeolites. Effects of synthesis conditions on the chemical environments of Ti species as well as catalytic activities of the resultant catalysts were systematically investigated. The obtained results demonstrated that the greatly enhanced catalytic performance of TS-1 zeolites was highly associated with the formation of mononuclear TiO_6 . This discovery paves the way for designed synthesis and catalytic applications of titanosilicate zeolites with active Ti sites.

Experimental

Preparation of conventional TS-1 (TS-1-C), active seeds and calcined seeds:

TS-1-C zeolite was synthesized from the starting gel with the molar composition of $\text{SiO}_2 : 0.0167\text{TiO}_2 : 0.4\text{TPAOH} : 1.5\text{CH}_3\text{CH}_2\text{OH} : 23.5 \text{H}_2\text{O}$ under hydrothermal conditions at 170 °C. Typically, tetrapropylammonium hydroxide (TPAOH) and deionized water were mixed completely, and then tetraethylorthosilicate (TEOS) was added dropwise to a mixture of H_2O and TPAOH under vigorous stirring, giving rise to a clear solution. Then, tetrabutyl orthotitanate (TBOT) and ethanol were added to this solution dropwise. After complete hydrolysis of TEOS and TBOT, the resulting solution was transferred into a Teflon-lined stainless steel autoclave and then crystallized in an oven at 170 °C for 1.5 h - 4 d under static condition. The obtained colloidal product was used as active seeds. After separation by centrifuging and drying at 80 °C in an oven overnight, followed by calcination at 550 °C for 6 h. The calcined product was used as calcined seeds.

Preparation of TS-1-AM and TS-1-CM:

TS-1 zeolites were synthesized from the starting gels with the molar compositions of $\text{SiO}_2 : (0.0667 - 0.0167) \text{TiO}_2 : 0.4\text{TPAOH} : 1.5\text{CH}_3\text{CH}_2\text{OH} : 23.5 \text{H}_2\text{O}$ under hydrothermal conditions at 170

°C. Typically, TPAOH (25 wt%) and deionized water were mixed completely, and then TEOS was added dropwise to a mixture of H_2O and TPAOH under vigorous stirring, giving rise to a clear solution. Then, tetrabutyl orthotitanate (TBOT) and ethanol were added to this solution dropwise. After complete hydrolysis of TEOS and TBOT, a certain amount of active seeds or calcined seeds (2 wt%, based on SiO_2) was added into the mixture under vigorous stirring. Finally, the resulting solution was transferred into a Teflon vessel and crystallized at 170 °C in a microwave reactor for 1 h under static condition. The sample synthesized via the combination of active seeds assistance and microwave irradiation was denoted as TS-1-AM. The sample synthesized via the combination of calcined seeds assistance and microwave irradiation was denoted as TS-1-CM.

Preparation of TS-1-A, TS-1-M:

As for TS-1-A and TS-1-M, they were prepared with the same synthesis procedure as described above while solely using active seeds assistance under conventional hydrothermal conditions (1h) and microwave irradiation conditions (1h), respectively.

Catalytic tests

The epoxidation of 1-hexene with H_2O_2 was carried out in a 25 mL two-necked round-bottom-flask equipped with a reflux condenser under vigorous stirring and at atmospheric pressure. In a typical run, 10 mL of methanol, 10 mmol of 1-hexene, 10 mmol of H_2O_2 (30 wt %) and 50 mg of the catalyst were mixed in the flask, and the reaction was run under magnetic stirring at 333 K. After the completion of the reaction, the liquid products were separated by centrifugation and analyzed with a gas chromatograph (Agilent 6890N), equipped with a 30 m capillary column (HP-5MS) and an FID detector using chlorobenzene as an internal standard. The conversion of 1-hexene and the selectivity of epoxides were calculated accordingly. All the products were confirmed by GC-MS (Thermo Fisher Trace ISQ).

In the recycling tests of the 1-hexene epoxidation reaction, the used catalyst was dried at 353 K overnight and calcined in air at 823 K for 6 h for the next use.

Results and discussion

By combining the active seeds assistance and microwave irradiation, highly catalytic active Ti species can be effectively created in well-crystallized TS-1 zeolite (denoted as TS-1-AM). In comparison, the conventional TS-1 (denoted as TS-1-C), the active seed-assisted conventional TS-1 (denoted as TS-1-A) and microwave-assisted TS-1 (denoted as TS-1-M) were prepared.

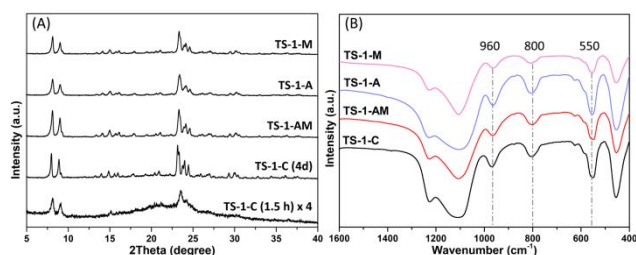


Fig. 1 XRD patterns (A) and FT-IR spectra (B) of different TS-1 samples.

According to the powder X-ray diffraction (XRD) analysis, conventional TS-1 zeolite normally requires 2-4 days crystallization (Fig. S1). In contrast, as shown in Fig. 1A, the TS-1 samples (TS-1-AM, TS-1-A and TS-1-M) crystallized in 1 hour already show much stronger diffraction peaks of **MFI** structure than TS-1-C (1.5 hours crystallization),³⁵ indicating both active seeds and microwave irradiation can accelerate the crystallization of TS-1 zeolites. Noteworthy, TS-1-AM (1h) exhibits almost same peaks intensity as conventional TS-1-C (4 days), which indicates the high crystallinity of TS-1-AM assisted by active seeds and microwave irradiation.

Fourier-transform infrared spectra (FT-IR) were used to characterize the formation of **MFI** structure and understand the level of titanium incorporated in the framework. As shown in Fig. 1B, the typical bands at 550 and 800 cm^{-1} appear in all TS-1 samples, which are attributed to the stretching vibration of double rings and $[\text{SiO}_4]$ units in **MFI** structure.³⁶ Moreover, the characteristic band at 960 cm^{-1} , which is assigned to the vibration of Si-O-Ti or Si-O bond perturbed by Ti atoms in the framework, is observed in the FT-IR spectra.^{37, 38} To evaluate the relative contents of framework titanium in different TS-1 zeolites, the intensity ratios of absorption band at 960 cm^{-1} to that at 800 cm^{-1} ($I_{960/800}$) are summarized in Table 1. Generally, a higher incorporation degree of framework Ti gives rise to a larger $I_{960/800}$. Compared with TS-1-C, TS-1-AM and TS-1-A, TS-1-M shows a lower $I_{960/800}$ value (0.62), indicating less Ti can be

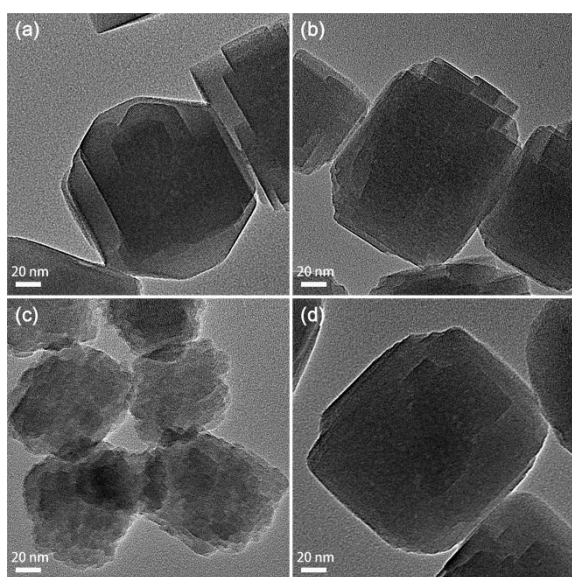


Fig. 2 TEM images of TS-1-C (a), TS-1-AM (b), TS-1-A (c), TS-1-M (d) zeolites.

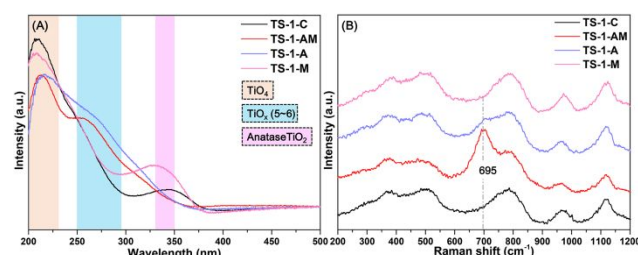


Fig. 3 UV-vis (A) and UV-Raman spectra (B) of TS-1-C, TS-1-AM, TS-1-A, TS-1-M zeolites.

properly inserted into the framework of TS-1 zeolite under the sole assistance of microwave irradiation.

According to transmission electron microscopy (TEM) and scanning electron microscopy (SEM) images (Fig. 2 and Fig. S2), TS-1-AM and TS-1-M possess the similar crystal size (*ca.* 150 nm) to TS-1-C. However, TS-1-A displays relatively smaller crystals with quite rough surface.

The nitrogen adsorption-desorption isotherms of different TS-1 zeolites are shown in Fig. S3. A clear hysteresis loop near saturation pressure ($0.8 < P/P_0 < 0.99$) is observed for all TS-1 samples, suggesting the existence of interparticle voids caused by the stacking of nano-sized TS-1 crystals. According to the textural properties summarized in Table S1, TS-1-A exhibits a smaller micropore surface area ($234.9 \text{ m}^2/\text{g}$) and micropore volume ($0.11 \text{ cm}^3/\text{g}$) than the well-crystallized TS-1 zeolites included TS-1-C, TS-1-AM, TS-1-M ($270\sim 280 \text{ m}^2/\text{g}$, $0.13 \text{ cm}^3/\text{g}$), revealing the incomplete crystallization of TS-1-A (1h). This finding is in accordance with the TEM result.

To probe the chemical environments of Ti species in different TS-1 zeolites, various spectroscopic techniques were employed. As shown in the ultraviolet-visible diffuse reflectance (UV-vis) spectra (Fig. 3A), two main absorption bands around 210 and 330 nm are observed for TS-1-C, indicating the existence of the tetrahedral-coordinated framework Ti species (TiO_4) and anatase TiO_2 .³⁹⁻⁴¹ Interestingly, a new absorption band around 250 - 290 nm appears in TS-1-A and TS-1-AM which is commonly attributed to the formation of high (penta- or octahedral) - coordinated Ti species.²¹ These results suggest that adding active seeds is beneficial for building high-coordinated Ti species. With regard to TS-1-M, the Ti species distribution is similar to that in TS-1-C, except a more significant characteristic band of anatase TiO_2 appears. Even though microwave assistance can greatly boost the crystallization rate of TS-1 zeolite, it will cause severe mismatch between the formation rate of **MFI** structure and the insertion rate of Ti ions.¹⁶ Consequently, more anatase TiO_2 will form during this process.

To get further insights on the high-coordinated Ti species, ultraviolet resonance Raman (UV-Raman) spectra of different TS-1 zeolites were also collected (Fig. 3B). It is reported that the Raman band at 695 cm^{-1} is associated with the so-called "mononuclear TiO_6 " based on DFT calculations.^{25, 28} Such characteristic band can be clearly found in TS-1-AM, notably, a weak shoulder band at 695 cm^{-1} is

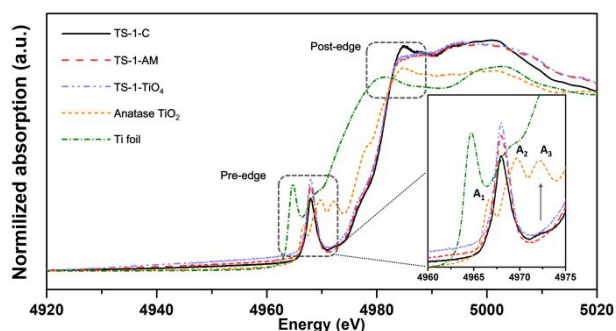


Fig. 4 Ti K-edge XANES spectra of different TS-1 samples, anatase TiO_2 and Ti foil reference.

also observable in TS-1-A. These results suggest that adding active seeds can induce the formation of “mononuclear TiO_6 ” during the crystallization of TS-1 zeolites and microwave irradiation can effectively boost the generation of TiO_6 in this process. Further analysis for the Ti species distributions in TS-1 zeolites based on X-ray photoelectron spectroscopy (XPS) is in good agreement with above results (Fig. S4).

The coordination environment and local structure of Ti species in TS-1 zeolites were further studied by taking XAS spectra at the Ti K edge. The X-ray absorption near edge structure (XANES) can probe the symmetry of Ti coordination structure in a qualitative manner by the comparison of the pre-edge peaks (around 4960 - 4980 eV) with those of reference materials,³¹ including Ti foil, anatase TiO_2 and pure tetrahedral-coordinated TS-1 zeolite -- TS-1- TiO_4 (Fig. S5). Generally speaking, the more symmetrical structure of Ti species leads to the more intense pre-edge peaks.^{42, 43} As shown in Fig. 4, the highest single peak can be observed in TS-1- TiO_4 which is due to the symmetrical structure of TiO_4 .⁴⁴ In the case of anatase TiO_2 , the pre-edge features give rise to three weak peaks denoted A_1 , A_2 and A_3 .⁴⁵ As for TS-1-AM, compared with TS-1- TiO_4 , the single pre-edge peak somewhat decreases which should be attributed to the formation of a part of distorted species (TiO_6). With respect to TS-1-C, the intensity of such peak further decreases which indicates a

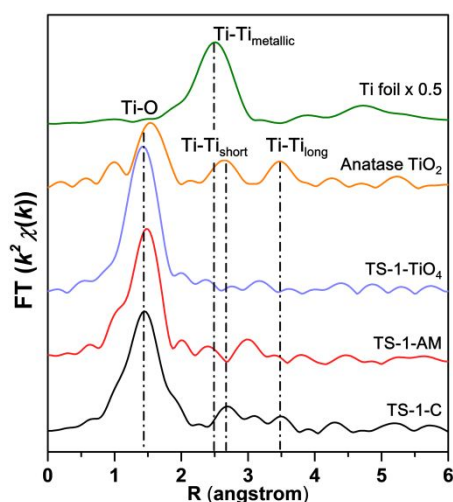


Fig. 5 Fourier transforms k^2 -weighted Ti EXAFS spectra in R-spacing of different TS-1 samples, anatase TiO_2 and Ti foil reference.

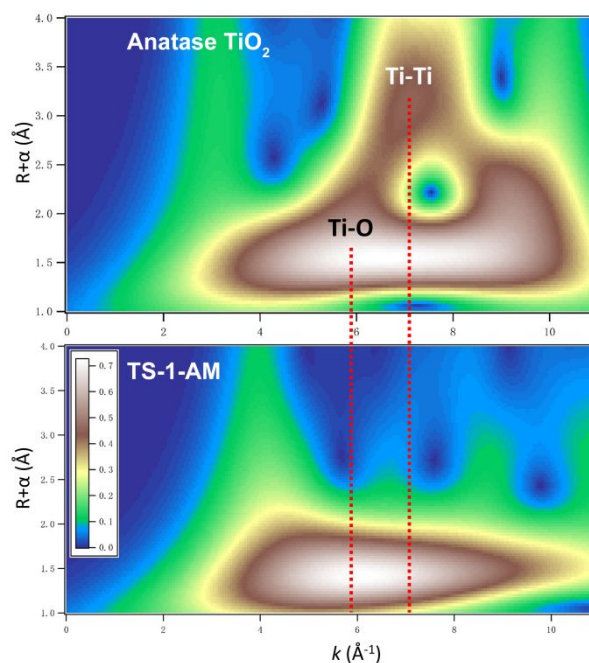


Fig. 6 Wavelet transforms (WT) of TS-1-AM and anatase TiO_2 . The WT contour plots are based on Morlet wavelets ($\kappa = 6$, $\sigma = 0.8$). The vertical dashed lines point out the k -space position of the Ti-O and Ti-Ti contributions.

more distorted Ti species formed. Meanwhile, a weak peak appears at the same position of A_3 in anatase TiO_2 , suggesting the existence of anatase TiO_2 in TS-1-C. In the post-edge region, TS-1- TiO_4 and TS-1-AM show much less distinct feature than those of TS-1-C and anatase TiO_2 . The lack of distinct feature in this area can be explained by the loss of long- and medium-range ordered structures. That is to say, Ti is more dispersed in TS-1- TiO_4 and TS-1-AM.

As shown in Fig. 5, the Fourier-transformed extended X-ray absorption fine structure spectra (FT-EXAFS) spectra of TS-1-AM show a major peak of Ti-O bond, while no obvious Ti-Ti bonds are detected, in sharp contrast to TS-1-C. These results directly confirm that all Ti atoms are isolated in TS-1-AM which is the most important feature of titanium silicate catalysts. Moreover, the best fit of the obtained EXAFS data (Fig. S6 and Table S2) reveals that the coordination number of Ti-O shell in TS-1-AM (4.3) is larger than that of TS-1- TiO_4 (4), which should be attributed to the formation of high coordinated TiO_6 species in TS-1-AM along with framework TiO_4 species.

The wavelet transform (WT)-EXAFS is a powerful method for separating backscattering atoms that provides not only a radial distance resolution but also resolution in k -space.³¹ As shown in Fig. 6, it can be observed that the WT maximum corresponding to the Ti-Ti shell is not shown for TS-1-AM in the interval from 2.5 to 3.7 Å, verifying the absence of Ti-Ti coordination. Therefore, the Ti atoms in TS-1 are homogeneously substituted into T sites of the **MFI** framework without any occupation of adjacent T sites in pairs. As a consequence, the local structure of newly detected TiO_6 can be solidly confirmed as a kind of mononuclear Ti species.

The change of coordination states of Ti species in TS-1 zeolites, i.e., before and after calcination, were addressed by

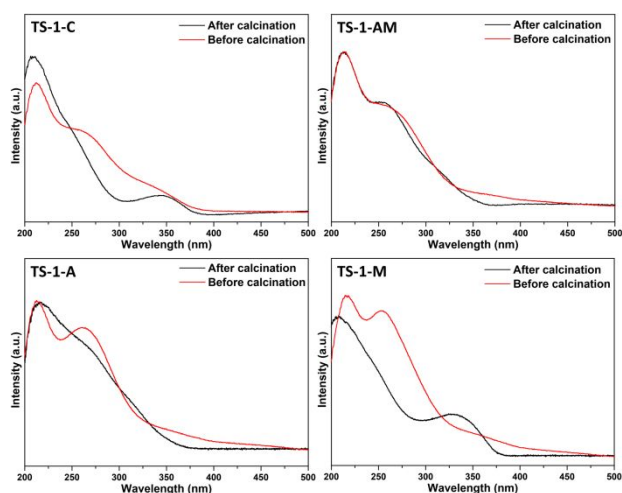


Fig. 7 UV-vis spectra of TS-1-C, TS-1-AM, TS-1-A, TS-1-M zeolites before and after calcination.

UV-vis spectra (Fig. 7). Interestingly, it seems that high coordinated Ti species exist in TS-1-C, TS-1-AM, TS-1-A, and TS-1-M samples before calcination, evidenced by the absorption band around 250 - 290 nm. According to the literature, such kind of Ti species is weakly coordinated by organic template molecules or water ligands.^{46, 47} No evident peak around 330 nm can be found in the spectra of samples before calcination, indicating the absence of anatase TiO₂ in as-synthesized TS-1 zeolites. After calcination, however, a significant broad band occurs around 330 nm in TS-1-C and TS-1-M. This might be due to that the high coordinated Ti species in TS-1-C and TS-1-M are not stable which may condense and aggregate to form anatase TiO₂ upon calcination.⁴⁸ For TS-1-A, it can be observed that after calcination the spectrum becomes broader, indicating that a part of high coordinated Ti species is unstable. Notably, the UV-vis spectrum of TS-1-AM remains almost unchanged upon calcination. It can be inferred that the high coordinated Ti species, which has been characterized as mononuclear TiO₆, is highly stable.

Furthermore, the formation process of such unique mononuclear TiO₆ species was investigated in depth (Fig. 8). The XRD pattern of active seeds barely shows the diffraction peaks of **MFI** structure (Fig. 8A). However, the characteristic band (550 cm⁻¹) of double rings of **MFI** structure appears in FT-IR spectrum (Fig. 8B), suggesting this colloidal state material is abundant in zeolitic fragments. An intense peak at 270 nm is detected in the UV-vis spectrum (Fig. 8C), demonstrating that

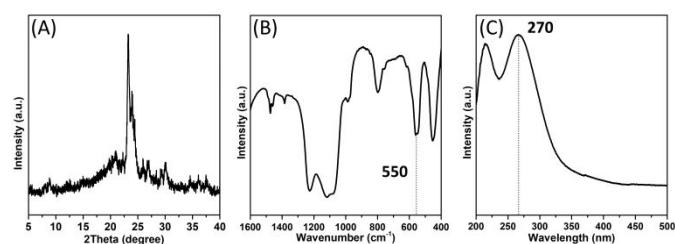


Fig. 8 The XRD pattern (A), FT-IR (B) and UV-vis (C) spectra of active seeds.

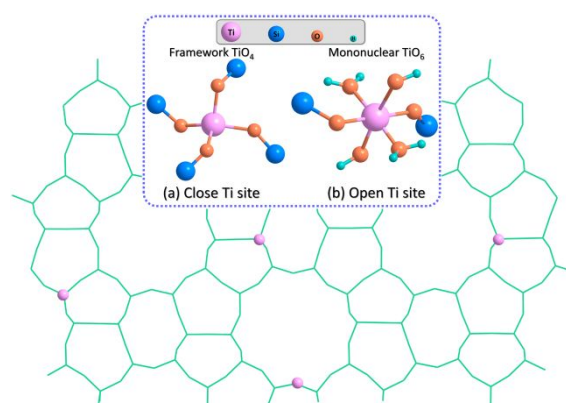


Fig. 9 Proposed titanium active sites in TS-1: (a) closed Ti site, (b) open Ti site.

plenty of high-coordinated Ti species exist in the active seeds. Such Ti species plays a crucial role in inducing the generation of mononuclear TiO₆ species. In addition, early literature reported that the Ti-O bond ($\Delta\chi=2.18$) is a better microwave absorber than the Si-O bond ($\Delta\chi=1.76$).⁴⁹ Thus, more high-coordinated Ti species can be strongly activated to form stable mononuclear TiO₆ under microwave irradiation. In comparison, we replaced active seeds with calcined seeds in such synthesis system. The resultant product (TS-1-CM) possesses high crystallinity and main framework TiO₄ distribution (Fig. S7, S8). However, the high-coordinated Ti species is absent in such catalyst. Compared with TS-1-AM, TS-1-CM exhibits lower catalytic activity in 1-hexene epoxidation reaction (Table S3). Therefore, calcined seeds cannot take effect on the generation of highly active mononuclear TiO₆ species in TS-1.

The epoxidation of 1-hexene was further employed to evaluate the catalytic properties of different TS-1 zeolites (Table 1). Elemental analysis by X-ray fluorescence spectrometer (XRF) shows that TS-1-AM (Si/Ti = 80) possesses relatively lower Ti-content than TS-1-C (Si/Ti = 70). However, the 1-hexene conversion over TS-1-AM shows significantly promotion than that over TS-1-C (TS-1-AM: 28.0 % vs. TS-1-C: 18.8%) and the selectivity of epoxide product for these two

Table 1. Epoxidation of 1-hexene over different TS-1 samples

	$I_{960/800}^a$	Si/Ti ^b	Conv. (%)	Sel. (%)		TON ^c
				epoxide	others	
TS-1-C	1.03	70	18.8	93.2	6.8	161
TS-1-AM	1.10	80	28.0	90.0	10.0	272
TS-1-A	0.98	87	12.3	94.7	5.3	131
TS-1-M	0.62	73	12.2	94.5	5.6	110

a. $I_{960/800}$ is used to estimate the relative content of framework Ti. b. The elemental compositions are determined by XRF; c. TON in mol (mol of Ti)⁻¹, turnover number per Ti site for 1-hexene conversion. Reactions conditions: catalyst 50 mg, 1-hexene 10 mmol, H₂O₂ 10 mmol, CH₃OH 10 mL, temp. 333 K, time 2 h. Others, 1-methoxyhexan-2-ol, 2-methoxyhexan-1-ol, 1,2-hexanediol.

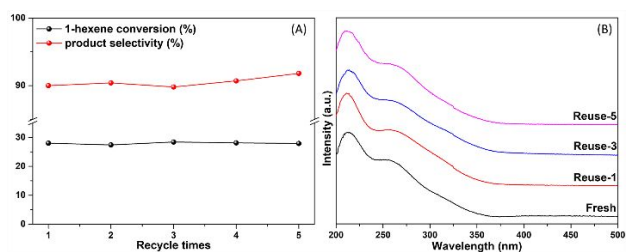


Fig. 10 Catalytic activity of 1-hexene epoxidation (A) and UV-vis spectra (B) of fresh and reused TS-1-AM.

catalysts stays at the same level. The turnover number (TON) values were calculated to further elucidate the intrinsic activity of the catalysts. TS-1-AM gives the TON of 1-hexene up to 272 which is almost 70% higher than that of TS-1-C (161). Furthermore, we found the catalytic activity of TS-1-AM is also higher than that of TS-1-TiO₄ which only contains the framework TiO₄ (Fig. S5 and Table S4). It is reported that the mononuclear TiO₆ species (open Ti sites) is more active than the framework TiO₄ species (close Ti sites) in alkenes epoxidation reactions (Fig. 9).²⁵ As proved above, the main difference between TS-1-TiO₄ and TS-1-AM lies in the mononuclear TiO₆ species. Therefore, such novel active Ti centers should be responsible for the promoted catalytic activity. In contrast, the catalytic properties of TS-1-A and TS-1-M are suppressed, which should be explained by the incomplete crystallization and high content of anatase TiO₂, respectively. In addition, the catalytic performance of highly crystalline TS-1-A crystallized for 4d is still poor due to the harmful anatase TiO₂ formed under the conventional crystallization condition (Fig. S9 and Table S4).

The catalytic performance of TS-1-AM with various Ti contents was also investigated (Fig. S10). With the increase of Ti content, the 1-hexene conversion gradually improves. However, when the ratio of Ti/(Si+Ti) is higher than 0.0124, the TON slightly decreases. Due to the highly catalytic active mononuclear TiO₆ species is a kind of open Ti sites, the content of accessible mononuclear TiO₆ might be limited. Therefore, the optimized Ti content of TS-1-AM zeolites is Ti/(Si+Ti) = 0.0093 - 0.0124.

The stability of TS-1-AM was investigated in 1-hexene epoxidation. As shown in Fig. 10A, the 1-hexene conversion and 1, 2-epoxyhexane selectivity of TS-1-AM stay almost the same after 5 times reuse. In addition, even after 5 time regeneration under calcination condition, the UV-vis spectra (Fig. 10B) demonstrates the highly active Ti species ($\lambda=260$ nm) in the used catalyst stays stable, without the formation of anatase TiO₂. Furthermore, XRD and FT-IR analysis indicate that TS-1-AM remains well-structured after the durability test (Fig. S11).

Conclusions

In conclusion, the one-step rapid synthesis of TS-1 zeolite with highly catalytic active Ti species has been achieved by introducing active seeds and microwave irradiation. Based on the UV-vis and UV-Raman spectra, the novel octahedral-coordinated Ti species (TiO₆) is presented in resultant TS-1

zeolites. The mononuclear state of TiO₆ species is further determined by X-ray absorption spectroscopy. Experimental studies reveal that adding active seeds can induce the formation of mononuclear TiO₆; on the other hand, the microwave irradiation will boost the generation of such TiO₆. The mononuclear TiO₆ species in the prepared TS-1 remain stable upon calcination, without the formation of anatase TiO₂. The TS-1 catalyst with mononuclear TiO₆ species exhibits outstanding catalytic activity and stability in 1-hexene epoxidation. This work offers a facile approach to modulate the coordination environment of Ti species in Ti-containing zeolites, which will enlighten the rational synthesis and catalytic application of titanasilicate zeolites with highly catalytic active Ti sites.

Conflicts of interest

There are no conflicts to declare.

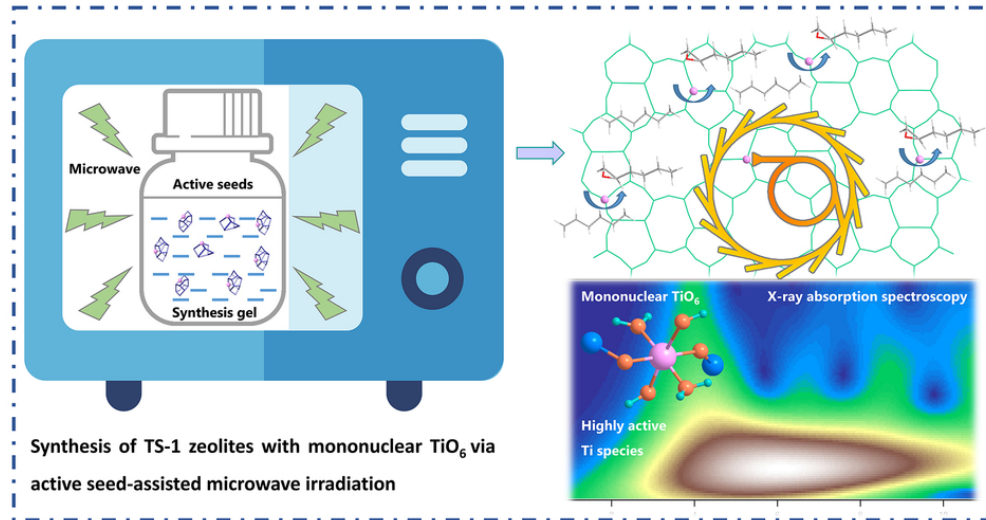
Acknowledgements

We thank the financial supports by the National Natural Science Foundation of China (Grant 21920102005, 21835002 and 21621001), the National Key Research and Development Program of China (Grant 2016YFB0701100), the 111 Project of (B17020). The APS was operated for the U.S. DOE Office of Science by Argonne National Laboratory, and the CLS@APS facilities (Sector 20) were supported by the U.S. DOE under Contract No. DEAC02-06CH11357, and the Canadian Light Source and its funding partners. Tianjun Zhang acknowledges the China Scholarship Council (CSC).

Notes and references

- 1 A. Corma, F. Rey, J. Rius, M. J. Sabater and S. Valencia, *Nature*, 2004, **431**, 287-290.
- 2 Z. Wang, J. H. Yu and R. R. Xu, *Chem. Soc. Rev.*, 2012, **41**, 1729-1741.
- 3 R. R. Xu, W. Q. Pang, J. H. Yu, Q. S. Huo and J. S. Chen, *Chemistry of zeolites and related porous materials*, John Wiley & Sons, (Asia) Pte Ltd, 2007.
- 4 M. G. CLERICI, G. Bellussi and U. Romano, *J. Catal.*, 1991, **129**, 159-167.
- 5 Y. Kuwahara, K. Nishizawa, T. Nakajima, T. Kamegawa, K. Mori and H. Yamashita, *J. Am. Chem. Soc.* 2011, **133**, 12462-12465.
- 6 L. Z. Wu, S. F. Zhao, L. F. Lin, X. P. Fang, Y. M. Liu and M. Y. He, *J. Catal.*, 2016, **337**, 248-259.
- 7 J. Kim, J. Chun and R. Ryoo, *Chem. Commun.*, 2015, **51**, 13102-13105.
- 8 N. Tsunoji, M. Opanasenko, Martin Kubu, J. Čejka, H. Nishida, S. Hayakawa, Y. Ide, M. Sadakane and T. Sano, *ChemCatChem.*, 2018, **10**, 2536-2540.
- 9 M. A. Mantegazza, G. Leofanti, G. Petrini, M. Padovan, A. Zecchina and S. Bordiga, *Stud. Surf. Sci. Catal.*, 1994, **82**, 541-550.
- 10 S. Inagaki, Y. Tsuboi, M. Sasaki, K. Mamiya, S. Park and Y. Kubota, *Green Chem.*, 2016, **18**, 735-741.
- 11 Y. Zuo, M. Liu, T. Zhang, C. G. Meng, X. W. Guo, C. S. Song, *ChemCatChem*, 2015, **7**, 2660-2668.
- 12 P. Wu, T. Tatsumi, T. Komatsu and T. Yashima, *J. Phys. Chem. B*, 2001, **105**, 2897-2905.

- 13 J. H. Ding and P. Wu, *Appl. Catal., A*, 2014, **488**, 86-95.
- 14 B. Tang, W. L. Dai, X. M. Sun, N. J. Guan, L. D. Li and M. Hunger *Green Chem.*, 2014, **16**, 2281-2291.
- 15 J. Přeč, *Catal. Rev.*, 2018, **60**, 71-131.
- 16 T. J. Zhang, X. X. Chen, G. R. Chen, M. Y. Chen, R. S. Bai, M. J. Jia and J. H. Yu, *J. Mater. Chem. A*, 2018, **6**, 9473-9479.
- 17 D. H. Wells, W. N. Delgass and K. T. Thomson, *J. Am. Chem. Soc.*, 2004, **126**, 2956-2962.
- 18 Y. Zuo, W. C. Song, C. Y. Dai, Y. P. He, M. L. Wang, X. S. Wang, X. W. Guo, *Appl. Catal., A*, 2013, **453**, 272-279.
- 19 A. Korzeniowska, J. Grzybek, W. Roth, A. Kowalczyk, P. Michorczyk, J. Čejka, J. Přeč and B. Gil, *ChemCatChem.*, 2018, **10**, 1-9.
- 20 X. Q. Fang, Q. Wang, A. M. Zheng, Y. M. Liu, Y. N. Wang, X. J. Deng, H. H. Wu, F. Deng, M. Y. He and P. Wu, *Catal. Sci. Technol.*, 2012, **2**, 2433-2435.
- 21 M. Sasaki, Y. Sato, Y. Tsuboi, S. Inagaki and Y. Kubota, *ACS Catal.*, 2014, **4**, 2653-2657.
- 22 K. Y. Leng, Y. Y. Sun, X. Zhang, M. Yu and W. Xu, *Fuel*, 2016, **174**, 9-16.
- 23 X. Q. Fang, Q. Wang, A. M. Zheng, Y. M. Liu, L. F. Lin, H. H. Wu, F. Deng, M. Y. He, P. Wu, *Phys. Chem. Chem. Phys.*, 2013, **15**, 4930-4938.
- 24 Y. Wei, G. Li, R. M. Su, H. Lu, H. C. Guo, *Appl. Catal., A*, 2019, **582**, 117108.
- 25 L. Z. Wu, X. J. Deng, S. F. Zhao, H. M. Yin, Z. X. Zhuo, X. Q. Fang, Y. M. Liu and M. Y. He, *Chem. Commun.*, 2016, **52**, 8679-8682.
- 26 L. Xu, D. D. Huang, C. G. Li, X. Y. Ji, S. Q. Jin, Z. C. Feng, F. Xia, X. H. Li, F. T. Fan, C. Li and P. Wu, *Chem. Commun.*, 2015, **51**, 9010-9013.
- 27 Y. Zuo, M. Liu, T. Zhang, L. W. Hong, X. W. Guo, C. S. Song, Y. S. Chen, P. Y. Zhu, C. Jayec and D. Fischer, *RSC Adv.*, 2015, **5**, 17897-17904.
- 28 Q. Guo, K. J. Sun, Z. C. Feng, G. N. Li, M. L. Guo, F. T. Fan, C. Li, *Chem. Eur. J.*, 2012, **18**, 13854-13860.
- 29 W. O. Parker and R. Millini, *J. Am. Chem. Soc.*, 2006, **128**, 1450-1451.
- 30 M. Signorile, V. Crocellà, A. Damin, B. Rossi, C. Lamberti, F. Bonino and S. Bordiga, *J. Phys. Chem. C*, 2018, **122**, 9021-9034.
- 31 J. Dong, H. L. Zhu, Y. J. Xiang, Y. Wang, P. F. An, Y. Gong, Y. X. Liang, L. M. Qiu, A. G. Zheng, X. X. Peng, M. Lin, G. T. Xu, Z. Y. Guo, D. L. Chen, *J. Phys. Chem. C*, 2016, **120**, 20114-20124.
- 32 A. C. Alba-Rubio, J. L. G. Fierro, L. León-Reina, R. Mariscal, J. A. Dumesic, M. López. Granados, *Appl. Catal., B*, 2017, **202**, 269-280.
- 33 Y. K. Hwang, J. S. Chang, S. E. Park, D. S. Kim, Y. U. Kwon, S. H. Jung, J. S. Hwang and M. S. Park, *Angew. Chem. Int. Ed.*, 2005, **44**, 556-560.
- 34 R. S. Bai, Q. M. Sun, Y. Song, N. Wang, T. J. Zhang, F. Wang, Y. C. Zou, Z. C. Feng, S. Miao and J. H. Yu, *J. Mater. Chem. A*, 2018, **6**, 8757-8762.
- 35 S. T. Du, F. Li, Q. M. Sun, N. Wang, M. J. Jia and J. H. Yu, *Chem. Commun.*, 2016, **52**, 3368-3371.
- 36 X. Gao, J. G. An, J. L. Gu, L. Li and Y. S. Li, *Microporous Mesoporous Mater.*, 2017, **239**, 381-389.
- 37 P. Ratnasamy, D. Srinivas and H. Knozinger, *Adv. Catal.*, 2004, **48**, 1-169.
- 38 M. Liu, Z. H. Chang, H. J. Wei, B. J. Li, X. Y. Wang and Y. Q. Wen, *Appl. Catal., A*, 2016, **525**, 59-67.
- 39 C. Liu, J. L. Huang, D. H. Sun, Y. Zhou, X. L. Jing, M. M. Du, H. T. Wang and Q. B. Li, *Appl. Catal., A*, 2013, **459**, 1-7.
- 40 N. Tsunaji, H. Nishida, Y. Ide, K. Komaguchi, S. Hayakawa, Y. Yagenji, M. Sadakane and T. Sano, *ACS Catal.*, 2019, **9**, 5742-5751.
- 41 J. Přeč, D. Vitvarová, L. Lupínková, M. Kubů, Martin and J. Čejka, *Microporous Mesoporous Mater.*, 2015, **212**, 28-34.
- 42 S. Bordiga, S. Coluccia, C. Lamberti, L. Marchese, A. Zecchina, F. Boscherini, F. Buffa, F. Genoni, G. Leofanti, G. Petrini and G. Vlaic, *J. Phys. Chem.*, 1994, **98**, 4125-4132.
- 43 S. Bordiga, F. Boscherini, S. Coluccia, F. Genoni, C. Lamberti, G. Leofanti, L. Marchese, G. Petrini, G. Vlaic and A. Zecchina, *Catal. Lett.*, 1994, **26**, 195-208.
- 44 H. K. D. Nguyen, G. Sankar and R. A. Catlow, *J. Porous Mater.*, 2017, **24**, 421-428.
- 45 F. Jin, C. C. Chang, C. W. Yang, J. F. Lee, L. Y. Jang and S. F. Cheng, *J. Mater. Chem. A*, 2015, **3**, 8715-8724.
- 46 F. Geobaldo, S. Bordiga, A. Zecchina, E. Giamello, G. Leofanti and G. Petrini, *Catal. Lett.*, 1992, **16**, 109-115.
- 47 L. Xu, D. D. Huang, C. G. Li, X. Y. Ji, S. Q. Jin, Z. C. Feng, F. Xia, X. H. Li, F. T. Fan, C. Li and Peng Wu, *Chem. Commun.*, 2015, **51**, 9010-9013.
- 48 P. Wu, T. Tatsumi, T. Komatsu and T. Yashima, *J. Phys. Chem. C*, 2001, **105**, 2897-2905.
- 49 Z. Sun, T. Li, G. Li, Y. H. Zhang and Y. Tang, *RSC Adv.*, 2017, **7**, 35252-35256.



79x42mm (300 x 300 DPI)